

Physical model test of reinforced flexible pavement

Kunakulsawat, V.

Director General, Department of Rural Road, Ministry of Transport, Thailand

Punthutaecha, K.

Civil Engineer, Bureau of Road Maintenance, Department of Rural Road, Ministry of Transport, Thailand

Youwai, S.

Assistant Professor, Department of Civil Engineering, King Mongkut's University of Technology Thonburi

Kongkitkul, W.

Lecturer, Department of Civil Engineering, King Mongkut's University of Technology Thonburi

Jongpradist, P.

Assistant Professor, Department of Civil Engineering, King Mongkut's University of Technology Thonburi

Maneetes, H.

Civil Engineer, Bureau of Road Construction, Department of Rural Road, Ministry of Transport, Thailand

Keywords: physical model, flexible pavement, geotextile

ABSTRACT: The distress problems for flexible pavement (FP) are mainly caused by underestimation of traffic volume and degrading of material properties. One of the economical methods to increase the overall performance, in particular, the long-term ones, of FP is to reinforce it with geosynthetic reinforcement. In this study, a series of scaled-down model tests were performed on FP and overlay either reinforced or unreinforced with geogrid or geocomposite layer, subjected to cyclic loading Shear strain distributions for sub-soil underneath the FP were determined by means of a photogrammetric method. From testing results it was observed that the permanent deformation of reinforced FP as well as shear strain of base layer below asphaltic concrete was significantly lower than those of non-reinforced FP.

1 INTRODUCTION

The main distress problems of asphaltic concrete in flexible pavement are rutting and fatigue from excessive traffic volume. One of the effective methods to reduced such distress problems is to reinforce the pavement with geosynthetic material in the base layer. ase layer. According to Bergado et al. (2001), the reinforcement material can increase the CBR value at the interface boundary of base and subbase layers. Perkins et al, (2005) concluded that the initial cost of construction for using the reinforcement is higher than the conventional method but the improvement of due to long-term behavior is much better than the unreinforced pavement. Kulkarni et al. (1997) using geosynthetic material (geotextiles and geogrid) in the field for maintenance (overlay) of Malharper-Pandharpur Road in India. The using geosynthetic materials can reduce the distribution of cracking in pavement. Especially, geogrid materials can increase the life time of pavement to 3 times when compared to that without reinforcement. Hoe et al, 2001 investigated the behavior of geosynthetic materials to use as reinforcement at under layer of asphalt concrete of flexible pavement by the model tests. From model test results, geosynthetic reinforcing materials can reduce the settlement of pavement structure.. However, there has been no comprehensive study investigating the strain developed in the

pavement layers when the overlay is reinforced using a geosynthetic. and reinforced overlay flexible pavement.

2 PHYSICAL MODEL

2.1 Testing material

The scale-down physical model for flexible pavement was employed to investigate the behaviors of reinforced pavement. The asphaltic concrete in this study was hot-mix with asphalt (AC60-70) content at 5 percent. The thickness of asphaltic concrete was 60 mm. the unit weight of asphaltic concrete was controlled at 21 kN/m³ and 18 kN/m³ for new pavement and damage pavement, respectively. The material for base layer of such flexible pavement was "KMUTT Sand". Firstly, sand was cleaned and produced the gradation in the range of standard sand, such as Toyoura sand and Ottawa Sand as shown in Fig. 1.

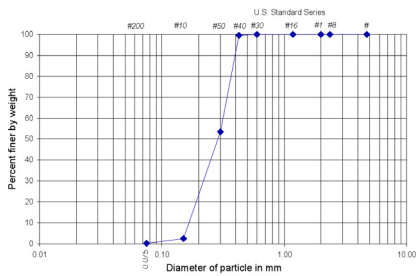


Fig.1 Gradation of sand for base layer of flexible pavement

Table 1 Properties of geotextile

Property	Test Standard	Unit	Value
Asphalt retention	Texas DOT Item 3099 ASTM D6140-97	kg/m ²	1.1
Tensile strength (md/ed)	-	kN/m	50 / 50
Elongation at break	ISO 3341	%	3
Strength at 2 % strain	-	kN/m	34 / 34
E-Modulus of the glass filaments	-	MPa	73,000
Mesh width of the glass filaments	-	mm	40 x 40
Mass per unit area	EN ISO 9864	g/m ²	300

Table 2 Properties of geogrid

Property	Test Standard	Unit	Value
Tensile strength (warp)	ISO 10319	kg/m	50
Tensile elongation (warp)	ISO 10319	%	4
Tensile strength (weft)	ISO 10319	kg/m	50
Tensile elongation (weft)	ISO 10319	%	4
Aperture size	-	Mm	20 x 20
Mass per unit area (g/m ²)	ISO 9864, ASTM D5261	g/m ²	335
Width	-	m	0.5 or 1.0
Length	-	m	50

Two types of geosynthetics were used in this study, which were non-woven geotextile and geogrid as shown their properties in Table 1 and Table 2. The material for geogrid and geotextile were made from fiber grass for resisting high temperature of hot-mix asphaltic concrete. To eliminate the stiffness effects of reinforcement, the stiffness of both reinforcement was similar.

2.2 Physical Model Tests

The physical model for plane-strain condition consisted of 2 parts, which were sand-box and loading system, as shown in Fig. 2. The side-wall of sand-box was made by transparent acrylic for monitoring deformation of base layer underneath the flexible pavement. The deformation was monitored by using LVDT, laser displacement transducer and photogrammetric method. The loading system was applied by using air pressure controlled by load obtained from load cell.

A large sand box having: 180 cm-wide x 40 cm-deep (σ_2 - direction) x 80 cm-high (Hirakawa, 2003) was used to prepare the scale-down model of FP structure. The side walls of the sand box, which were transparent, were lubricated by 0.3 mm-thick latex rubber sheets smeared with 50 μ m-thick high-vacuum silicone grease (Tatsuoka et al., 1984). Then, KMUTT sand was pluviated into the sand box through air (Miura and Toki, 1982) so that the relative density of about higher than 95 % was achieved. FP specimens were prepared by compacting hot-mixed asphalt at controlled target densities into a mold made of steel frames and plywood. Subsequently, FP specimen was placed on the surface of KMUTT sand which was horizontal leveled in advance.

A rough rigid footing having a width (B) of 6 cm was centrally placed on the top of FP specimen. The vertical compression applied to the footing was achieved by an automated pneumatic loading system (Fig. 2). A load cell and a LVDT were used to measure the axial load and the axial compression of the footing, respectively. Two laser displacement sensors were installed at $1B$ and $2.5B$ from the center to measure the vertical deflection of the FP specimen during a test. In addition, markers of 52 x 40 points in respectively horizontal and vertical directions with spacing of 5 mm were printed on the latex rubber sheet for subsequent photogrammetric analysis (Kongkitkul et al., 2007).

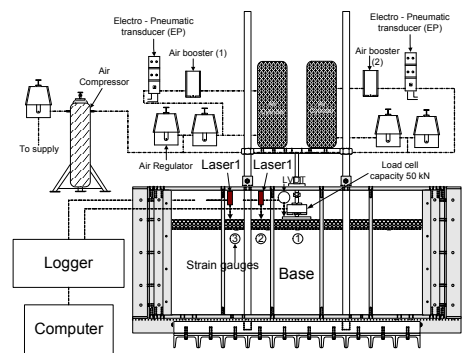


Fig. 2 Physical model test

Table 3 Testing program

Testing Code	Description
NPNO	New pavement without reinforcement
NPGT	New pavement with geotextile
NPGG	New pavement with geogrid
DNO	Overlay reinforced pavement without reinforcement
DGT	Reinforced overlay with geotextile
DGG	Reinforced overlay pavement with geogrid
DGGGT	Reinforced overlay pavement with geogrid and geotextile

2.3 Testing Program

The testing program consisted of 7 cases for new pavement and overlay as shown in Table 3. The thickness of asphaltic concrete was 60 mm placed on sand base layer. For overlay case, the thickness of damage asphaltic concrete layer was 30 mm. The reinforcement was placed on the damage asphaltic layer following by 30 mm thick of new hot mix asphaltic concrete. Loading was applied by cyclic loading with the frequency of 8 minute per each loop. The loading amplitude was 400 kPa

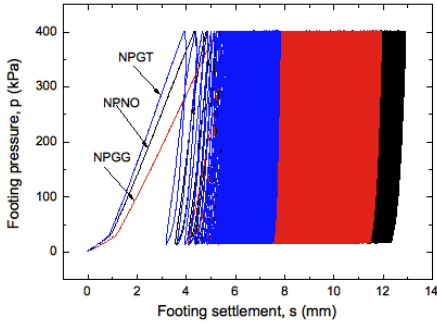


Fig. 3 Load-settlement curve of cyclic loading for reinforced pavement with different type of reinforcement.

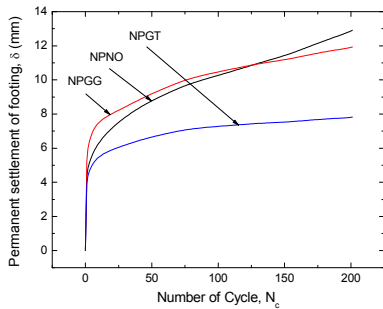


Fig. 4 Relationship between permanent deformation and number of cycle for different type of reinforced flexible pavement

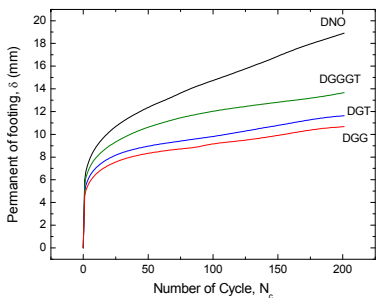


Fig. 5 Relationship between permanent deformation and number of cycle for overlay reinforced flexible pavement

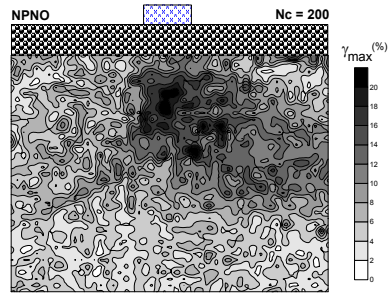


Fig. 6 Shear strain of base layer below non-reinforced flexible pavement

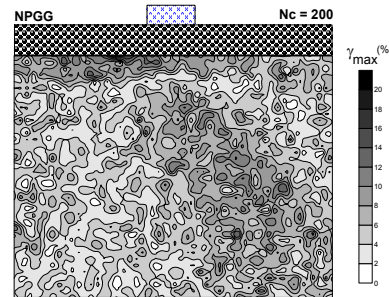


Fig. 7 Shear strain of base layer below flexible pavement reinforced with geotextile

3 TESTING RESULTS

The relationships between permanent deformation and applied pressure for the new flexible pavement were shown in Fig. 4. Due to hardening behaviors of asphaltic concrete and sand subjected to cyclic loading, the permanent deformation remarkably reduced when number of loading applied was beyond 20 loops. The permanent deformation of new pavement reinforced with geotextile was significantly lower than reinforced flexible pavement with geogrid and non-reinforced sections. For geogrid reinforcement, due to lower bound between asphaltic concrete and itself, the permanent deformation was approximately similar to non-reinforced case.

The strain field under flexible pavement at 200 loops of cyclic loading for non-reinforced and geotextile reinforced cases were illustrated in Figs. 6 and 7. The reinforcement was significantly reduced the shear strain sand underneath the flexible pavement. Thus, the adding reinforcement in flexible pavement was not only reduced the rutting problems but also reduce the fatigue crack problem of asphaltic concrete due to reduction of settlement of base layer.

Figs. 6 to 8 show the distribution of maximum shear strain, γ_{max} , mobilized when $N_c = 200$ underneath the FP and overlay specimens unreinforced and reinforced with geotextile, respectively. It may

be seen that γ_{\max} localized at about center and the depth which is twice of the FP specimen's thickness in the case of unreinforced FP while uniform distribution of γ_{\max} was observed in the case of geogrid-reinforced FP. In addition, γ_{\max} at some locations in the case of unreinforced FP were already in the post-peak regime or even in the residual state of the stress-strain relation. That is, it is likely from Fig. 6 that, if N_c were continued, localization of γ_{\max} is further developed to progressively form a shear band or bands, resulting in the foundation failure of the FP structure. Therefore, it is clearly seen that the geogrid-reinforced FP is more effective than the unreinforced one when transferring the vertical stress from the vertical compression of the footing to the underneath foundation.

For case of overlay, the reinforcement can reduce the permanent deformation of reinforced pavement as shown in Fig. 5. The permanent deformation of flexible pavement reinforced with geogrid was lower than the case that using geotextile as reinforcement. The permanent deformation of the case of using both geogrid and geotextile was higher than the case that employed the single type of reinforcement. It might be caused from the slippage between geogrid and geotextile. From the strain field obtained from physical model, the reinforcement can reduce the deformation of sand underneath the flexible pavement.

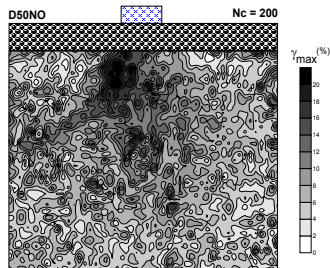


Fig. 8 Shear strain of base layer below non-reinforced overlay

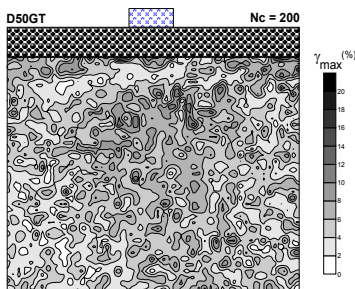


Fig. 9 Shear strain of base layer below reinforced overlay with geotextile

4 CONCLUSION

The physical model testing of flexible pavement and overlay with different types of reinforcement has been conducted subjected to cyclic loading. The permanent deformation for each loop of cyclic loading tended to reduce with number of cycle. The permanent deformation of flexible pavement and overlay noticeably reduced with employment of reinforcement. For flexible pavement, the permanent deformation of FP reinforced with geotextile was significantly lower than those reinforced with geogrid. For overlay, the permanent deformation for overlay reinforced with geogrid and geotextile was approximately identical. The shear strain of sand layer of reinforced flexible pavement was lower than the case without reinforcement.

REFERENCES

- Bergado, D. T., Youwai, S., Hai, C. N. and Voottipreux, P. 2001. Interaction of Nonwoven Needle-Punched Geotextiles Under Axisymmetric Loading Conditions with Application to Reinforced Unpaved Roads, *Geotextiles and Geomembranes*, 19: 299-328.
- Perkins, S. W., Bowders, J. J., Christopher, B. R. and Berg R. R. 2005. Geosynthetic Reinforcement for Pavement Systems: US Perspectives, *Geotechnical Special Publication ASCE (30) 155*: 1-15.
- Perkins, S. W., Bowders, J. J., Christopher, B. R. and Berg R. R. 2005. Geosynthetic Reinforcement for Pavement Systems: US Perspectives, *Geotechnical Special Publication (130-142)*: 3039-3063.
- Kulkarni, A. W., Shah, M.H, Hai, Decate, M.N. and Adhikari, A. 1998. Strengthening of road in black cotton soil region and improvement of overlay against reflective and fatigue cracking using, *Geosynthetic Asia*: 19-31.
- Hoe, I. Ling, Zheng, Liu, 2001, Performance of Geosynthetic-Reinforced Asphalt Pavements. *Geotechnical and Geoenvironmental Engineering*, ASCE: 177-184.
- Tatsuoka, F., Molenkamp, F. Torii, T. and Hino, T. 1984. "Behaviour of lubrication layers of platens in element test", *Soils and Foundations*, Vol.24, No.1, pp.113-128.
- Miura, S. and Toki, S. (1982): "A simple preparation method and its effect on static and cyclic deformation strength properties of sand", *Soils and Foundations*, Vol.22, No.1, pp.61-77.
- Kongkitkul, W., Tatsuoka, F. and Hirakawa, D. (2007): "Rate-dependent load-strain behaviour of geogrid arranged in sand under plane strain compression", *Soils and Foundations*, Vol.47, No.3, pp.473-491.
- Hirakawa, D. (2003): "Study on residual deformation characteristics of geosynthetic-reinforced soil structures", *Ph.D. Thesis*, University of Tokyo (in Japanese).